

Original Study

Open Access

Monika Podwórna*, Jacek Grosel

Optimizing DVA placement using evolutionary algorithms for dynamic beam loading

<https://doi.org/10.2478/sgem-2025-0011>

received October 3, 2024; accepted March 28, 2025.

Abstract: Dynamic vibration absorbers (DVAs) are used to suppress the excessive structural response due to dynamic loading. To maximize their effectiveness, the placement and characteristics of DVAs need to be carefully chosen. To address this challenge, a methodology that enables this task to be accomplished by means of an evolutionary algorithm is presented in this paper. A beam subjected to a sequence of forces with random amplitudes, which move at random time instances with a constant velocity, is considered. The beam has either one or a set of two arbitrarily located DVAs. The loading is modeled using a filtered Poisson process, while the DVAs are modeled as single-degree-of-freedom (SDOF) systems. It is shown that the proposed algorithm can serve as a powerful tool when selecting an arrangement of DVAs, in turn effectively mitigating any undesired structural response. Moreover, the optimization of DVAs leads to the asymmetry of the absorber's position along the length of a bridge's beam. The obtained results can be used to evaluate the correctness of calculations conducted for the purpose of assessing structural damping requirements.

Keywords: Dynamic Vibration Absorber; Stochastic Load; Genetic Algorithm.

1 Introduction

The problem of reducing the level of vibrations in various constructions has been considered for a very long time. The dynamic vibration absorber (DVA) and tuned mass damper (TMD) have a long history, as they were invented in the previous century. The concept was first applied

by Frahm [1] as a spring-supported mass. The theory for DVA (the first concept involved a viscous damper added parallel to the linear spring) was presented by Ormondroyd and Den Hartog [2], with a detailed discussion later being developed by Den Hartog [3]. The first concept is considered as the standard model of DVA.

Construction objects are subjected to aging processes and other changes and influences during their life cycle, which, after some time, result in the occurrence of their technical, functional, and environmental wear. When analyzing the phases of the life cycle of a building object, it can be noticed that the operation and maintenance (O&M) phase is the longest phase [4], especially in the case of bridges. Moreover, the O&M phase is determined in various ways. The application of DVAs has a special role in civil engineering, which is due to the fact that they can be used not only during a construction's design (the design and development phase), but also later to modify the structure (the O&M phase).

Bridge structures face challenges associated with their quality and design and are exposed to the occurrence of disaster risks such as earthquakes, typhoons, floods, landslides, corrosion deterioration, and overloading. Proper maintenance is required for the safety of bridges, as well as for them to remain in good condition [5]. Therefore, so many researchers are analyzing the problem of structures that may be vulnerable to excessive vibrations caused by dynamic loadings, that is wind [6], earthquakes [7], human action [8], and traffic [9], especially high-speed trains [10]. Moreover, absorbers can be used to prevent large vibration amplitudes that occasionally appear, for example, those caused by geotechnical works [11].

DVAs work on the principle of transferring the vibration energy from the primary structure to the auxiliary systems [12]. Passive TMD absorbers have been known as Voigt-type DVAs for more than a hundred years. In turn, DVAs are available in various physical forms. TMDs can be made of solid materials, but can also be based on liquids (tuned liquid damper) – [13], active mass damper [14], semi-active mass damper [15], and hybrid mass damper [16]. The essential limitation of TMD is that a large oscillating mass is required to achieve significant

*Corresponding author: **Monika Podwórna**, Wrocław University of Science and Technology, Wyb. Wyspiańskiego 27, 50-370 Wrocław, Poland, E-mail: monika.podworna@pwr.edu.pl; ORCID: 0000-0002-1967-0384

Jacek Grosel, Wrocław University of Science and Technology, Wyb. Wyspiańskiego 27, 50-370 Wrocław, Poland; ORCID: 0000-0002-4815-1719

vibration reduction. This characteristic has limited the use of TMDs in, among other things, the automotive and aerospace sectors [17]. Some papers describe the nonlinear properties of main structures or the stiffness of the TMD system [18]. New varieties of absorbers have also been invented. For example, a TMD with a negative stiffness element – called the KDamper – is a novel passive vibration isolation and damping concept, based essentially on the optimal combination of appropriate stiffness elements, which include a negative stiffness element. Compared to the traditional TMD, the KDamper can achieve better isolation characteristics, without the need of additional heavy masses [17]. Another variation of the new type of absorber can be a three-element TMD (T-TMD), which can be used as an effective passive control device. According to [19], it can be an effective strategy to minimize the maximum structural responses of multi-story buildings under seismic excitations. Another type of absorber – the TMD inerter (TMDI) – can also be used for this purpose [20].

The main objective in the design of an absorber is to enable it to have optimum parameters. Due to the fact that the mass ratio of DVA to the primary structure is usually a few percent, the principal parameters of DVA are its tuning ratio (i.e., the ratio of the DVA's eigenfrequency to the natural frequency of the primary structure) and damping ratio [3]. Most studies assume that the load process is deterministic, and that it is harmonic. There are more and more papers that analyze stochastic loading. Many researchers have focused on analysis of the effectiveness of DVAs applied to beams that are excited by moving loads. For example, Wang et al. [26] analyzed three basic modeling procedures of vehicles: moving force, moving mass, and moving suspension mass. The problem of optimization of absorbers connected with a bridge beam, and loaded by a moving force, has been considered in many papers [21-26]. The authors analyze nonlinear vibration absorbers [27], translational supports and rotational joints [28], or absorbers that are attached at equal intervals under a bridge [29].

The problem of choosing the optimal parameters for a set of damping absorbers that reduce the random vibrations of a beam subjected to a sequence of moving forces with a constant velocity is studied in this paper. Every force is regarded as a random variable. Moreover, the inter-arrival times of moving forces are also regarded as random variables. The stochastic properties of the load are modeled by means of a filtered Poisson process. The problem was solved using the idea of a dynamic influence function [30]. Several optimization criteria, based on the expected values and variance of the beam's response, were

considered. The authors analyzed solutions for a beam with one and two independently installed absorbers. However, the developed methodology allows the task to be solved with any number of absorbers.

2 Formulation of the problem and general solutions

2.1 The issue

The damped vibrations of a simply supported Euler-Bernoulli beam of finite length L with n_a absorbers fitted at points $x_{a1}, x_{a2}, \dots, x_{an_a}$ subjected to a sequence of moving forces with a constant velocity v is considered.

The vibrations of the beam are described by the equation:

$$EI \frac{\partial^4 w(x,t)}{\partial x^4} + c \frac{\partial w(x,t)}{\partial t} + m \frac{\partial^2 w(x,t)}{\partial t^2} + \sum_{i=1}^{n_a} r_i(t) \delta(x - x_{ai}) = \sum_{k=1}^{N(t)} A_k \delta[x - v(t - t_k)], \quad (1)$$

where EI denotes the flexural stiffness of the beam, m denotes the mass per unit length of the beam, c is the damping coefficient, $\delta(\cdot)$ denotes the Dirac delta function, and $r_i(t)$ is the force response of the i -th absorber acting on the beam. The reaction of an absorber on the beam can be derived from the equilibrium of the absorber, that is, the reaction $r_i(t)$ between the beam and the i -th absorber is given by the following equation:

$$r_i(t) = M_{ai} \frac{d^2 q_{ai}(t)}{dt^2}, \quad (2)$$

where M_{ai} and q_{ai} are mass and displacement of the i -th absorber, respectively.

For a finite, simply supported beam, the boundary conditions have the following forms:

$$w(0, t) = w(L, t) = 0, \quad (3)$$

$$\left. \frac{\partial^2 w(x, t)}{\partial x^2} \right|_{x=0} = \left. \frac{\partial^2 w(x, t)}{\partial x^2} \right|_{x=L} = 0 \quad (4)$$

The model of traffic is a set of random moving forces with a constant velocity v . The amplitudes A_k (see Fig. 1) are assumed to be random variables, which are both mutually independent and independent of the random instants t_k .

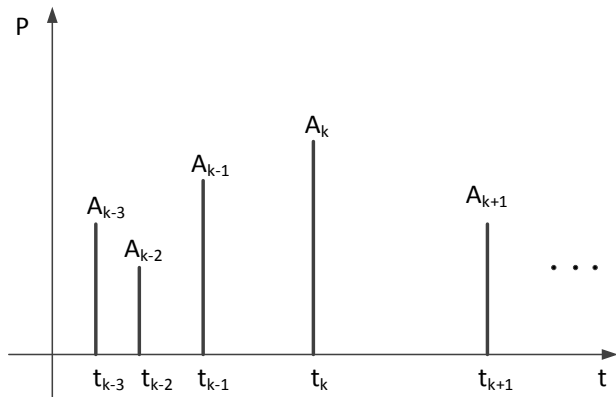


Figure 1: The model of the load.

It is assumed that the expected values $E[A_k]=E[A]=const$ are known. Random times t_k constitute a Poisson process $N(t)$ with parameter λ . Parameter $\lambda>0$ is the intensity of the Poisson process and is equal to the average number of forces per unit of time.

Let us introduce two dynamic influence functions – $H_1(x,t)$ and $H_2(x,t-L/v)$ [30]. Function $H_1(x,t)$ is the response of the beam at time t ($0 \leq t \leq L/v$) to a moving force equal to unity ($A_k=1$), and function $H_2(x,t-L/v)$ is the response of the system without excitation, but with non-zero initial conditions (the force has already left the beam). These influence functions satisfy the following differential equations:

$$EI \frac{\partial^4 H_1(x,t)}{\partial x^4} + c \frac{\partial H_1(x,t)}{\partial t} + m \frac{\partial^2 H_1(x,t)}{\partial t^2} + \sum_{i=1}^{n_a} r_i(t) \delta(x - x_{ai}) = \delta(x - vt), \quad (5)$$

$$EI \frac{\partial^4 H_2(x,t-\frac{L}{v})}{\partial x^4} + c \frac{\partial H_2(x,t-\frac{L}{v})}{\partial t} + m \frac{\partial^2 H_2(x,t-\frac{L}{v})}{\partial t^2} + \sum_{i=1}^{n_a} r_i \left(t - \frac{L}{v} \right) \delta(x - x_{ai}) = 0, \quad (6)$$

and appropriate boundary conditions and initial conditions:

$$H_1(x,0) = \frac{\partial H_1(x,t)}{\partial t} \Big|_{t=0} = 0, \quad (7)$$

$$H_2(x,0) = H_1 \left(x, \frac{L}{v} \right), \quad \frac{\partial H_2(x,t)}{\partial t} \Big|_{t=0} = \frac{\partial H_1(x,t)}{\partial t} \Big|_{t=\frac{L}{v}}. \quad (8)$$

where x_{ai} denotes the i -th absorber location on the beam.

The deflection of the beam $w(x,t)$ is counted at arbitrary time t , and none of the force locations are known. It can be written in the Stieltjes integral [30]:

$$w(x,t) = \int_{t-\frac{L}{v}}^t A(\tau) H_1(x,t-\tau) dN(\tau) + \int_{t_b}^{t-\frac{L}{v}} A(\tau) H_2 \left(x, t - \tau - \frac{L}{v} \right) dN(\tau). \quad (9)$$

The expected value of the random function $w(x,t)$ amounts to [30]:

$$E[w(x,t)] = E[A] \lambda \int_{t-\frac{L}{v}}^t H_1(x,t-\tau) d\tau + E[A] \lambda \int_{t_b}^{t-\frac{L}{v}} H_2 \left(x, t - \tau - \frac{L}{v} \right) d\tau, \quad (10)$$

whereas the variance amounts to [30]:

$$\sigma_w^2(x,t) = E[A^2] \lambda \int_{t-\frac{L}{v}}^t H_1^2(x,t-\tau) d\tau + E[A^2] \lambda \int_{t_b}^{t-\frac{L}{v}} H_2^2 \left(x, t - \tau - \frac{L}{v} \right) d\tau. \quad (11)$$

Symbol $E[\cdot]$ denotes the expected value of the quantity in the brackets, v_A is the coefficient of variation, and $E[A^2]=E^2[A](1+v_A^2)$. The above general solution will be used to optimize the absorber's parameters. For transient vibration, we assume $t_b=0$, and for steady state, $t_b=-\infty$. In the last case, equations (10) and (11) have the following forms:

$$E[w(x,\infty)] = E[A] \lambda \int_0^{\frac{L}{v}} H_1(x,\tau) d\tau + E[A] \lambda \int_{-\infty}^{\frac{L}{v}} H_2 \left(x, t - \tau - \frac{L}{v} \right) d\tau = E[A] \lambda E[w] \quad (12)$$

$$\sigma_w^2(x,\infty) = E[A^2] \lambda \int_0^{\frac{L}{v}} H_1^2(x,\tau) d\tau + E[A^2] \lambda \int_{-\infty}^{\frac{L}{v}} H_2^2 \left(x, t - \tau - \frac{L}{v} \right) d\tau = E[A^2] \lambda \sigma[w] \quad (13)$$

2.2 Determination of the dynamic influence function

In the case of a simply supported beam, one can look for dynamic influence functions in the form of sine series:

$$H_1(x, t) = \sum_{n=1}^{\infty} y_{1n}(t) \sin \frac{n\pi x}{L}, \quad (14)$$

$$H_2\left(x, t - \frac{L}{v}\right) = \sum_{n=1}^{\infty} y_{2n}\left(t - \frac{L}{v}\right) \sin \frac{n\pi x}{L}. \quad (15)$$

After substituting expressions (13, 14) into Eqs (5, 6), and using the orthogonality method while at the same time taking into consideration the first j eigenforms, the following sets of ordinary equations can be obtained:

$$\begin{aligned} \frac{d^2 y_{1n}(t)}{dt^2} + 2\alpha \frac{dy_{1n}(t)}{dt} + \omega_n^2 y_{1n}(t) + \\ + \sum_{i=1}^{n_a} r_i(t) \sin \frac{n\pi x_{ai}}{L} = \frac{2}{mL} \sin \frac{n\pi vt}{L}, \end{aligned} \quad (16)$$

$$\begin{aligned} \frac{d^2 y_{2n}(t)}{dt^2} + 2\alpha \frac{dy_{2n}(t)}{dt} + \\ + \omega_n^2 y_{2n}(t) + \sum_{i=1}^{n_a} r_i(t) \sin \frac{n\pi x_{ai}}{L} = 0, \end{aligned} \quad (17)$$

where $n = 1, 2, \dots, j$, $2\alpha = \frac{c}{m}$, $\omega_n^2 = \left(\frac{n\pi}{L}\right)^4 \frac{EI}{m}$. The initial conditions for functions $y_{1n}(t)$ and $y_{2n}(t)$ result directly from conditions (7) and (8).

2.3 Absorber equations

The vibrations of the single degree of freedom (SDOF) i -th absorber attached to the beam at point X_{ai} are described by the following equation:

$$\begin{aligned} M_{ai} \frac{d^2 q_{ai}(t)}{dt^2} + c_{ai} \left[\frac{dq_{ai}(t)}{dt} - \frac{dH_i(x_{ai}, t)}{dt} \right] + \\ + k_{ai} [q_{ai}(t) - H_{\vartheta}(x_{ai}, t)] = 0, \end{aligned} \quad (18)$$

where c_{ai} and k_{ai} is the damping coefficient and stiffness of the i -th absorber, respectively.

After taking into account (14) or (15) and the j first eigenforms, the vibrations have the form

$$\begin{aligned} \frac{d^2 q_{ai}(t)}{dt^2} + 2\alpha_{ai} \left[\frac{dq_{ai}(t)}{dt} - \sum_{n=1}^j \frac{dy_{\vartheta n}(t)}{dt} \sin \frac{n\pi x_{ai}}{L} \right] + \\ + \omega_{ai}^2 [q_{ai}(t) - \sum_{n=1}^j y_{\vartheta n}(t) \sin \frac{n\pi x_{ai}}{L}] = 0 \end{aligned} \quad (19)$$

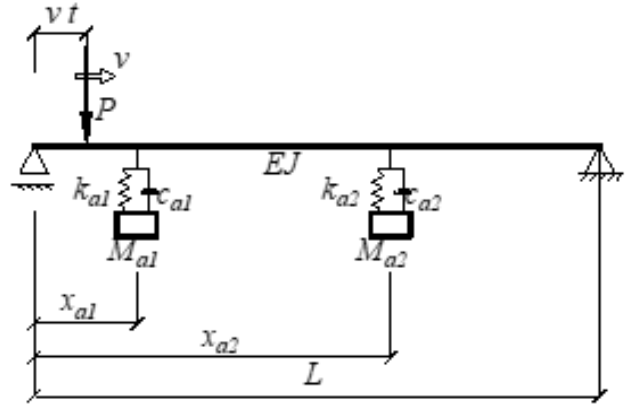


Figure 2: The model of the analyzed system ($n_a=2$).

$$\text{where } 2\alpha_{ai} = \frac{c_{ai}}{M_{ai}}, \omega_{ai}^2 = \frac{k_{ai}}{M_{ai}} \text{ and } \vartheta = \begin{cases} 1 & \text{for } t \leq \frac{L}{v} \\ 2 & \text{for } t > \frac{L}{v} \end{cases}.$$

2.4 The model

In literature, various ways of installing a set of absorbers can be found, such as two absorbers connected in a parallel manner, two absorbers connected as a series and installed at one point to a bridge beam [31], or the same absorbers that are attached at equal intervals under a bridge beam [29]. This paper focuses on a bridge beam with two independently installed absorbers.

For the model consisting of two absorbers (see Fig. 2), three separate systems of ordinary differential equations are obtained (Eq. 20), for which solutions are achieved by numerical integration using Wolfram Mathematica [32]. As a standard, this software uses the Runge–Kutta method, in turn automatically selecting the integration step. In the calculations, the maximum integration step was limited to one-thousandth of the passing time:

$$\begin{cases} EI \frac{\partial^4 w(x,t)}{\partial x^4} + c \frac{\partial w(x,t)}{\partial t} + m \frac{\partial^2 w(x,t)}{\partial t^2} + \sum_{i=1}^2 M_{ai} \frac{d^2 q_{ai}(t)}{dt^2} \delta(x - x_{ai}) = \sum_{k=1}^{N(t)} A_k \delta[x - v(t - t_k)] \\ \frac{d^2 q_{a1}(t)}{dt^2} + 2\alpha_{a1} \left[\frac{dq_{a1}(t)}{dt} - \sum_{n=1}^j \frac{dy_{\vartheta n}(t)}{dt} \sin \frac{n\pi x_{a1}}{L} \right] + \omega_{a1}^2 [q_{a1}(t) - \sum_{n=1}^j y_{\vartheta n}(t) \sin \frac{n\pi x_{a1}}{L}] = 0 \\ \frac{d^2 q_{a2}(t)}{dt^2} + 2\alpha_{a2} \left[\frac{dq_{a2}(t)}{dt} - \sum_{n=1}^j \frac{dy_{\vartheta n}(t)}{dt} \sin \frac{n\pi x_{a2}}{L} \right] + \omega_{a2}^2 [q_{a2}(t) - \sum_{n=1}^j y_{\vartheta n}(t) \sin \frac{n\pi x_{a2}}{L}] = 0 \end{cases} \quad (20)$$

$$\text{where } \vartheta = \begin{cases} 1 & \text{for } t \leq \frac{L}{v} \\ 2 & \text{for } t > \frac{L}{v} \end{cases}.$$

3 The evolutionary algorithm

The authors of [33] confirm that natural computing methods are good at optimizing the properties of an absorber. They used the method that was previously presented by Storn and Price [34] and wrote the following

conclusion: “Numerical results demonstrate that the TMD systems designed by the differential evolution (DE) algorithm are very effective in reducing the multi resonant peaks of continuous bridges under moving train loads.”

The algorithm used in the presented calculations combines elements of the genetic algorithm and evolutionary strategies. Both approaches belong to a large family of the so-called natural computing, which uses selection, reproduction, and mutation mechanisms inspired by the biological process of evolution. In the biological evolutionary process, environmental pressure acts on a given population of individuals, in turn causing natural selection, that is, survival and reproduction of the best adapted. In natural computing, the problem to be solved is placed in the environment in which the population of individuals lives. Everyone represents a potential (possible) solution to the problem. As in the biological process, the evolutionary algorithm creates progressively better solutions. Like with organisms living on earth, a certain population can be distinguished in computing, that is, the number of living individuals (in computing: the number of computing objects) or the successive generations (in computing: the successive iteration). The concepts of parents and children (computational objects of iteration/generation “g” and “g+1”), chromosomes (a set of parameters describing a computational object), genotypes, phenotypes, alleles, etc. are also transferred to the field of algorithms.

The basic structure of genetic algorithms is presented in Figure 3 [35, 36].

Classical genetic algorithms use binary notation, whereas evolutionary programs use floating point notation. In evolutionary programs, a parent generation of d_p members produces d_o offspring. Afterward, d_b best-fit individuals are selected from the $d_p + d_o$, population, $d_p = d_b$. In genetic algorithms, d_b descendants are selected from a population of d_b ; the selection is a random selection with repetition, in which the better-matched individuals are more likely to reproduce. The procedure for selecting the best match is deterministic in evolutionary programs (objective function) and random in genetic algorithms, although better-matched individuals obviously have a higher probability of being selected. The evolutionary strategies (mutation and crossover probabilities) in genetic algorithms are fixed, and in evolutionary programs, they are variable.

The used algorithm belongs to the group of evolutionary programs, although some modifications that can be found in genetic algorithms were also applied. The scheme of this algorithm is shown in Fig. 4.

```

procedure
  begin
    g=0
    determine the initial population P(g)
    evaluate population P(g)
    while (not condition_of_stop_is_fullfield) do
      begin
        g = g +1
        select P(g) from P(g - 1)
        change P(g)
        evaluate P(g)
      end
    end
  
```

Figure 3: The basic structure of genetic algorithms.

- Step 1. create an initial generation $g=0$, generation size $d_p + d_o$
- Step 2. check if the end condition is met,
 - if yes → end of computation, solution is best $[P(g)]$
 - if not → go further
- Step 3 evaluate generation $P(g)$ by selecting d_p best individuals
- Step 4. from the d_p individuals selected earlier, create d_o new individuals
 - a. draw two individuals $\{X_\alpha, X_\beta\}$ from which a new individual will be created, the parental individuals are drawn with equal probability
 - b. for each inherited parameter, draw whether the parameter is taken from an individual X_α or X_β , the draw is made with equal probability
 - c. for each inherited parameter draw (with probability ξ) whether the parameter (par) is subject to mutation, if a parameter with the value of pairs has been drawn for mutation modify it to the value of $par+N(0, \sigma)$, $N(0, \sigma)$ is a normal distribution with mean zero and standard deviation σ
 - d. if the mutated parameter has a value outside the allowed range, a penalty is added to the value of $P(g)$, i.e. $P(g)=P(g)+value_of_the_penalty$
- Step 5. $g = g + 1$, return to Step 2

Figure 4: The scheme of the genetic algorithm.

Notes to Fig. 4:

- Generation $P(g=0)$ was created purely at random;
- Best $[P(g)]$ is the best adapted individual from the population $P(g)$;
- The end condition was the number of iterations (total number of generations). Other variants of the end condition were also tested. The very frequently used condition in iterations – stop if $|best[P(g)] - best[P(g-1)]| \leq \varepsilon$ (ε adopted difference between successive solutions) – does not work for genetic or evolutionary algorithms because a change in the solution can occur after many generations of no change (Fig. 5, where stagnant solutions can be observed for more than 100 generations). The following numbers of changes were tested: 100, 300, 500, 1000, and 2000 generations,

- and in most cases, the value of 300 generations was used;
- The evaluation function was the minimum expected value or standard deviation;
 - A descendant individual inherits every single parameter from parent X_α or parent X_β with equal probability, and it is possible that a descendant inherits all parameters from only one parent;
 - The probability of mutation was constant and equal to $\xi=1/2$. This is the most significant difference between the algorithm used here and the evolutionary algorithm. In evolutionary algorithms, there is always a mutation, that is, $\xi = 1$. The used approach is that of genetic algorithms, where the occurrence of mutations is random. Thanks to the used approach, a solution was obtained in fewer iterations. Compare, for example, book [36], where the author recommends using a low probability of mutation (inversely proportional to the population size);
 - The size of the mutation was determined by the parameter $N(0, \sigma)$, in which the value of σ was taken either as a constant in the calculations (e.g., 0.2, 0.5, 0.75) or as a variable that was decreasing with the next generation;
 - The *value_of_the_penalty* increases the value of $P(g)$ to such a significant degree that the penalized individual is bound to come last in the order described in Step 3.

An immanent feature of natural computing is that only an approximate solution is obtained. The algorithm may get “stuck” in some “local” solution, thus the “global” solution remains unachieved. Taking advantage of the fact that the structure under consideration is symmetrical, analyzing the passage of the force from the left to right support (“→”) should produce a symmetrical solution with respect to when the force passes from the right to the left side (“←”). The parameters of the absorbers obtained from the two solutions (“→” and “←”) can, therefore, be matched in pairs (ξ -th solution from “→” and η -th solution from “←”), so that the parameters of the absorbers are identical and the attachment points to the primary structure are symmetrical with respect to the center of the beam:

$$\begin{aligned} \text{par}(\xi, \text{“} \rightarrow \text{”}) &\approx \text{par}(\xi, \text{“} \leftarrow \text{”}) \\ x_a(\xi, \text{“} \rightarrow \text{”}) + x_a(\eta, \text{“} \rightarrow \text{”}) &\approx L \end{aligned} \quad (21)$$

How close the above formulas are to the exact solution, rather than approximate equality, allows the quality of the solution to be assessed. Based on how the above formulas

are met, the quality of the solution can be assessed precisely.

4 Numerical analysis and results

4.1 The model

The model of the structure refers to a road bridge with a suspended platform equipped with municipal technical infrastructure [37]. It is a reinforced concrete beam bridge with a span of $L=30$ m, in which the first eigenfrequency $\omega_s=4$ rad/s. In the numerical calculation, $j = 7$ was assumed. In the study, two indicators were analyzed: different positions of the absorbers $x_{ai} \in (0.25L; 0.75L)$ and one parameter of the absorber – the tuning ratio $\kappa_{ai} = \omega_{ai} / \omega_s$ ($0 \leq \kappa_{ai} \leq 5$). $E[A]$, $E[A^2]$, and λ have constant values for the homogeneous Poisson process. It was assumed that the vehicle traffic moves at a constant velocity v which was compared to the critical speed adopted according to the well-known formula ($v_{cr} = \pi v (EI/mL^2)$). The conclusions of [37] show that the critical speed does not cause the greatest deviations – a structure behaves least favorably when vehicles travel at speeds in the range of $v \in (0.6v_{cr}; 0.9v_{cr})$. After a broader analysis [38] of the measures of variability, it was noted that the responses are not symmetrical, that is, on the side where vehicles enter the bridge, all measures of variability are slightly smaller, especially the variance. Previous research did not consider the direction of travel, as the authors assumed symmetrical responses. Paper [38] proved that this assumption was wrong. In this regard, previous papers [30, 37, 38] are the reason for the search for an optimal position, regardless of the direction of travel. Therefore, the position of two absorbers was studied and the bridge was crossed in two directions. In previous papers [30, 37, 38], several optimization criteria, based on the expected values and variance of the beam’s response determined in the study, were considered. The current study shows the possibility of optimization by means of evolutionary algorithms.

It is obvious that higher vibration control efficiency can be achieved when the mass of an absorber increases. However, as the enhancement of the TMD mass causes more static deflection, and can also change the dynamic properties of the main system, the value of the TMD mass ratio should be chosen while considering all the aspects of the structural design. It should not be greater than 10% [39]. Therefore, in this paper, the constant mass parameter μ_{ai} was assumed to be equal to 0.1.

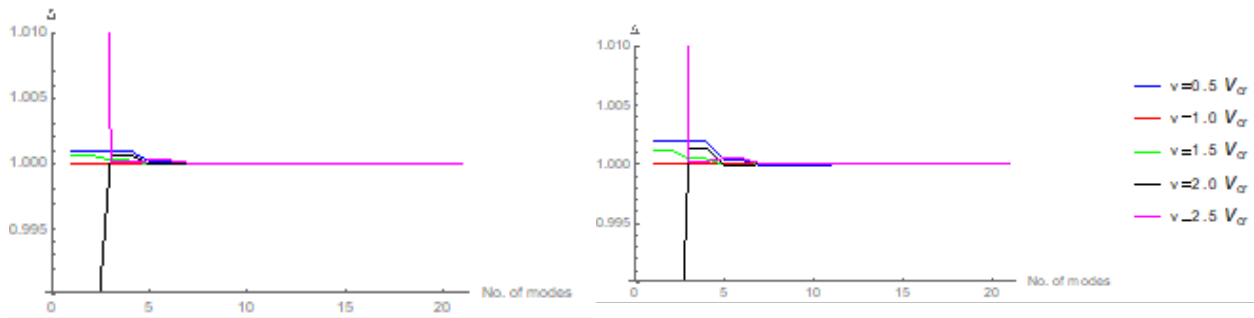


Figure 5: The Δ plot in the case of: a) $E[w(0.5L,t)]$, b) $\sigma[(0.5L,t)]$

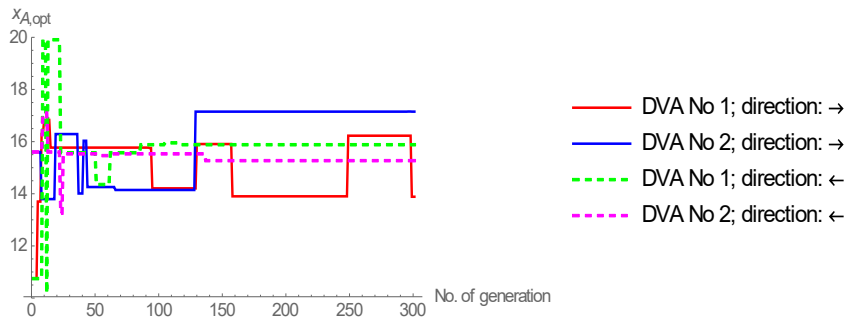


Figure 6. The optimal position of two absorbers $x_{ai} \in (0.25L; 0.75L)$ for two different directions of traffic moving with the constant velocity $v=0.8 v_{cr}$ for the adjustment function – the minimum of the expected value of deflection functions in the middle span of the bridge’s beam $E[w]$.

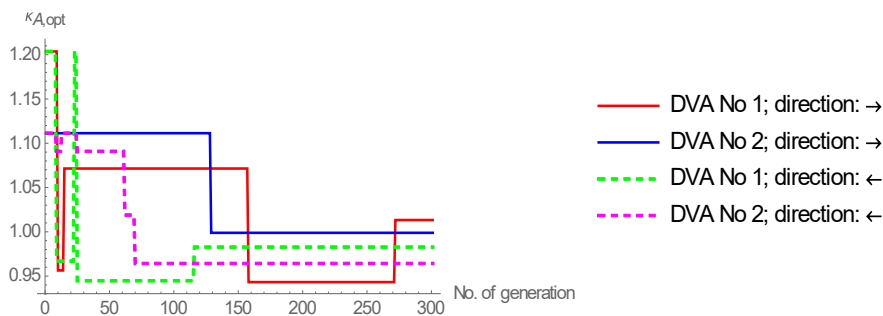


Figure 7: The optimal parameter $\kappa_{ai} = \omega_{ai} / \omega_s$ of two absorbers for two different directions of traffic moving with the constant velocity $v=0.8 v_{cr}$ for the adjustment function – the minimum of the expected value of deflection functions in the middle span of the bridge’s beam $E[w]$.

4.2 The size of the calculation base

The simply supported beam of length L and flexural stiffness EI is loaded with force P_1 . Force P_1 moves with the constant velocity v . The starting point for the force is the extreme supporting point of the beam (right support or left support), which corresponds to the direction of the force’s movement (left direction or right direction, respectively).

The dynamic problem was solved using the Galerkin method, and therefore, the first step was to analyze the

size of the approximation base. The effect of the size of the approximation base (the number of eigenforms considered in the solution) on the expected value $E(w)$ and standard deviation $\sigma(w)$ of the displacements in $1/4$, $1/2$, and $3/4$ of the span was studied.

The effect of the size of the approximation base was analyzed for base sizes ranging from 1 to 21. For further evaluations, it was assumed that the solutions obtained for a base size equal to 21 (r_{21}) are exact solutions. The

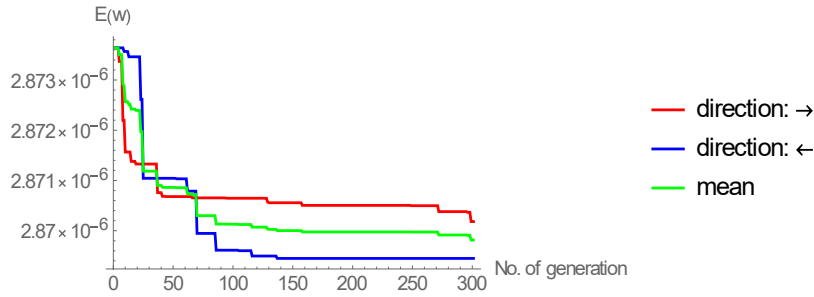


Figure 8: The adjustment function – the minimum of the expected value of deflection functions in the middle span of the bridge’s beam $E[w]$.

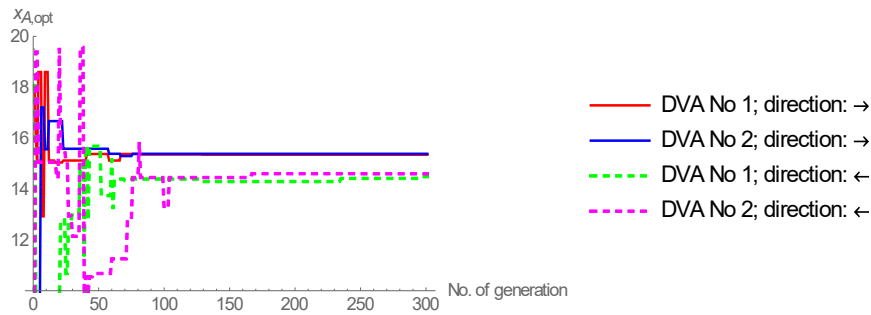


Figure 9. The optimal position of two absorbers $x_{ai} \in (0.25L; 0.75L)$ for two different directions of traffic moving with the constant velocity $v=0.8 v_{cr}$ for the adjustment function – the minimum of the standard deviation of deflection functions in the middle span of the bridge’s beam $\sigma[w]$.

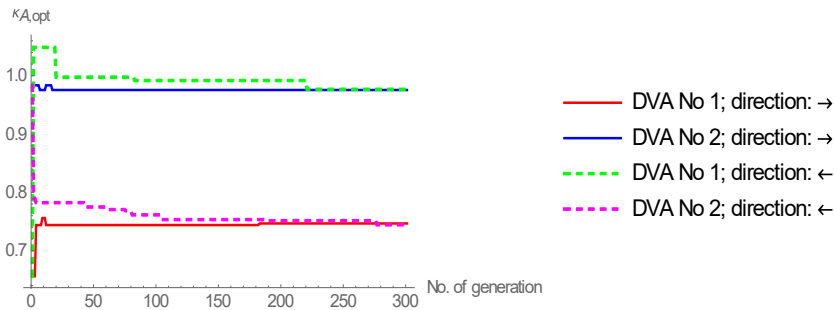


Figure 10: The optimal parameter $\kappa_{ai} = \omega_{ai}/\omega_s$ of two absorbers for two different directions of traffic moving with the constant velocity $v=0.8 v_{cr}$ for the adjustment function – the minimum of the standard deviation of deflection functions in the middle span of the bridge’s beam $\sigma[w]$.

relative precision for solutions obtained in the case of the base size of $k(r_k)$ was defined as:

$$\Delta = \frac{r_k}{r_{21}} \tag{21}$$

The following graphs show the Δ plot for $E(w)$ and $\sigma(w)$ at five different travel speeds. The accuracy of the solution is practically insensitive to the position of the section being analyzed and only slightly sensitive to the calculated quantity – $E(w)$ or $\sigma(w)$. Differences do not exceed one

per mille. The greatest impact was seen in the case of the travel speed of the force. The fastest convergence was obtained in the case of $v = 1.0 v_{cr}$, in which a solution with a relative error of less than 0.0001 was obtained using only four eigenmodes (base size equal to 4). The other speeds ranked in order of convergence were $v = 1.5 v_{cr}$, $2.0 v_{cr}$, $2.5 v_{cr}$ and $0.5 v_{cr}$. The smallest convergence occurred for the speed $v = 0.5 v_{cr}$. In this case, a solution with a relative error of less than 0.0001 was obtained using seven eigenmodes (base size equal to 7). This size of the calculation base was adopted for further calculations.

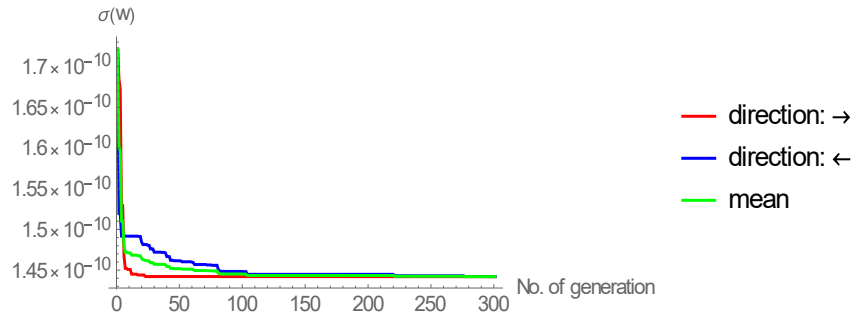


Figure 11: The adjustment function – the minimum of standard deviation of the deflection functions in the middle span of the bridge’s beam $\sigma[w]$.

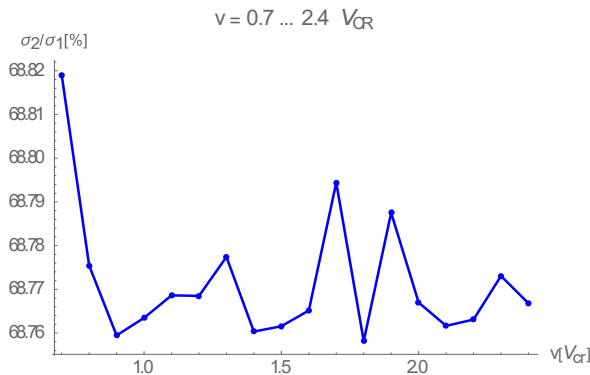


Figure 12: Comparison of the system’s response when applying one and two absorbers for different velocity $v=0.7 \div 2.4 v_{cr}$ for the adjustment function – the minimum of the standard deviation.

4.3 Results

Figure 6 demonstrates the optimal position of two absorbers for two different directions of traffic moving with the constant velocity $v=0.8 v_{cr}$. Similarly, Figure 7 shows the optimal value of the tuning ratio κ_{ai} for each absorber. The adjustment function is meant to minimize the expected value of deflection functions in the middle span of the bridge’s beam (see Fig. 8). Similar results were obtained for forces moving at speeds $v=0.9 v_{cr}$ and $v=v_{cr}=137.5 \text{ km/h}$.

Figures 9 and 10 present the optimal position of two absorbers for two different directions of traffic moving with the constant velocity $v=0.8 v_{cr}$ and the optimal value of parameter κ_{ai} for each absorber. The adjustment function is meant to minimize the standard deviation value of the deflection functions in the middle span of the bridge’s beam (see Fig. 11). It is clear from the diagrams that the positions of the two absorbers overlap, and that this optimum position of the double absorber is asymmetrical. This is an important premise for analyzing the feasibility of absorbers with two oscillating masses.

Similar results were obtained for forces moving at a constant velocity equal to the critical speed for this bridge.

Figures 6–13 show the results for 300 generations. It was determined that there is too poor convergence for the adjustment functions with regards to the expected value of deflection functions in the middle span of the bridge beam, but this convergence was sufficient for the standard deviation. Three hundred generations are also sufficient for analyzing results for a single absorber, regardless of the adjustment function.

The effectiveness of using two absorbers instead of one absorber while maintaining the same active mass in the absorbers was analyzed ($\sum M_{ai} = \text{const}$). When one absorber was analyzed, its mass was 10% of the total mass, and in the case of two absorbers, each had a mass equal to 5% of the total mass. The velocity was expressed by the critical speed of the passage of the force, and it ranged from 70% to 240% of the critical speed. The results are shown in Figure 12, where the ratio of the response (standard deviation of the mid-beam deflection) obtained for two absorbers (σ_2) to the response obtained when using one absorber (σ_1) is shown. It can be seen that the use of two absorbers (when compared to one) reduces the magnitude of the standard deviation by more than 30%.

Figure 13 shows the location of a single absorber (green line) or two absorbers (blue and red lines) with regards to the speed of the passage of the force through the beam. The asymmetry of the attachment of the absorbers can be seen – in the case of a single absorber, the minimum value of the attachment ordinate is 15.18 m, the maximum value is 15.25 m, and the average value is 15.20 m. For two absorbers, the minimum values are 15.22 and 15.23 m, the maximum values are 15.48 and 15.88 m, and the average values are 15.36 and 15.50 m. The results obtained for one absorber are less variable. The standard deviation for the data shown in Figure 13 is 0.016 m and for two absorbers, the values are 0.147 and 0.080 m, respectively.

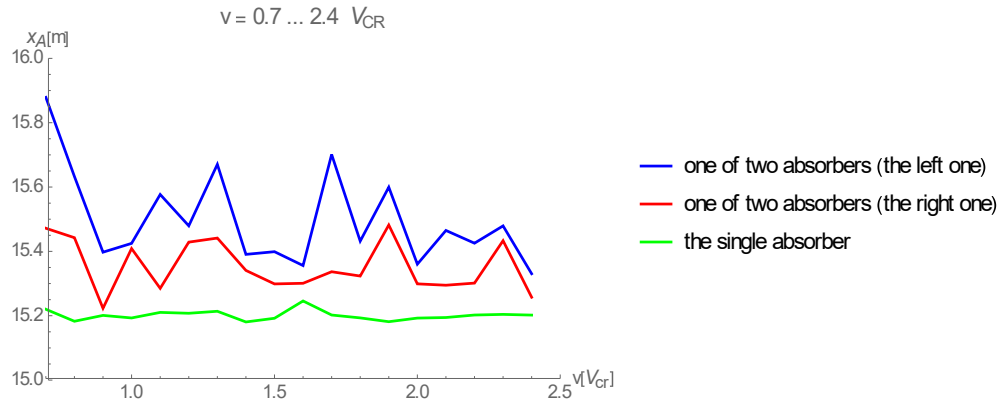


Figure 13: The optimal position of one or two absorbers $x_{ai} \in (0.25L; 0.75L)$ for different velocity $v = 0.7 \div 2.4 v_{cr}$ for the adjustment function – the minimum of the standard deviation of deflection functions in the middle span of the bridge’s beam $\sigma[w]$.

It should be noted that there is a qualitative change in the solution for one absorber when compared to the use of two absorbers. If two absorbers are used, the asymmetry of the solution and the degree of tuning of the absorbers increases. The mounting points of the absorbers are shifted behind half of the beam in the direction of the force’s movement. For one absorber, the average kappa tuning parameter ($\kappa_{ai} = \omega_{ai} / \omega_s$) is 0.78, and for two absorbers, the values are 0.82 and 0.90.

5 Discussion and comments

The method of verifying calculations, which is described in Section 3, allows for the assessment of the results shown in Figures 9 and 10 as being close to optimal (when using heuristic methods, e.g., evolutionary methods, we are never sure about the optimality of the results). In turn, the results shown in Figures 6 and 7 can be evaluated as being unsatisfactory and require further calculations (e.g., by increasing the number of generations). It is worth noting that the adjustment function in Figures 9 and 10 aims to minimize the value of the standard deviation of the deflection function in the middle span of the bridge’s beam $\sigma[w]$. In Figures 6 and 7, the adjustment function aims to minimize the expected value of the deflection function in the middle span of the bridge’s beam $E[w]$. The conducted analysis confirms the previous conclusion [37] that for optimizing the absorber, the variance is better than the expected value of deflection functions in the middle span of the bridge’s beam.

Weber & Feltrin [40] presented the following disadvantages of TMDs: (a) the mass requirements are significant when compared to the total mass of the structure and (b) environmental factors and uncertainty

in material behavior can lead to gradual upsetting of the system, resulting in a loss of its damping properties and effectiveness.

Based on the optimization criteria presented in previous papers [30, 37, 38] (minimization of the expected value and variance), the optimal parameters of one absorber with regards to its use are: $\mu_a = M_a / m_L \in (5\%; 15\%)$ and $\kappa_a = \omega_a / \omega_s \in (0.5; 2.5)$, whereas the optimal place of installing the absorber is $x_{ai} \in (0.4L; 0.6L)$. For this reason, attention was focused on two absorbers that are characterized by having a constant parameter $\mu_{a1} = \mu_{a2} = 0.05$ and a variable parameter $\kappa_{a1} = \kappa_{a2} \in (0.5; 2.5)$, as well as a different location along the length of the beam (within $x_{ai} \in (0.25L; 0.75L)$). It was determined that the variance of deflection of the center of the bridge’s beam should be taken into account when optimizing the absorber – the smaller the variance, the better the tuned absorber.

The analyzed absorbers’ location along the length of the bridge’s beam has confirmed earlier findings. It was found that the optimal location for each of the two absorbers is slightly asymmetric and within the range of $x_{ai} \in (0.45L, 0.58L)$. However, in the case of a single absorber, its optimal location is also asymmetric and within the range of $x_a \in (0.49L, 0.59L)$. A result consistent with the study of Samani & Pellicano [25] was obtained: the optimal location for the nonlinear damper is at the location of the absolute maximum deflection of the beam ($d = 0.53L$), and for the linear damper, it is at $d = 0.55L$.

In practice, an absorber with a frequency similar to the structure’s frequency ($\kappa \approx 1$) is most often used. The performed analysis shows that the optimal parameter κ_{ai} is equal to 0.95 for both absorbers. The optimal range is $\kappa_{ai} \in (0.74; 1.02)$ for a set of two absorbers and $\kappa_{ai} \in (0.87; 1.13)$ for a single device.

6 Conclusions

The obtained results confirm the validity of the use of natural calculation when solving optimization problems in civil engineering. Moreover, the idea of checking the correctness of calculations by using the symmetry of the system was confirmed by the achieved results.

The attenuation efficiency of two absorbers is higher than that of a single absorber. Moreover, the parameters (κ_{ai} , x_{ai}) of each of the two absorbers are significantly different from those of a single absorber. This result indicates the need for further research, especially if one takes into account the presence of two force streams (forces coming from the right and left).

The results presented in this paper confirm a certain asymmetry in the optimal positioning of absorbers. The next stage of the study will involve the optimization of absorbers loaded with a force stream that travels simultaneously from the left to the right and from the right to the left side of a bridge beam. The possibility of using “double” or “multiple” absorbers, that is, absorbers with two or more degrees of freedom, is also an issue that requires further research.

References

- [1] Frahm H., *Device for damping vibrations of bodies*. United States Patent (1911), 3576-3580.
- [2] Ormondroyd J., Den Hartog J.P., *The theory of the dynamic vibration absorber*, Transactions of ASME, Journal of Applied Mechanics 50 (1928), 9–22.
- [3] Den Hartog J.P., *Mechanical Vibrations*, 4th ed., Dover, New York, 1985.
- [4] Podwórna, M., *The aging of a building versus its life cycle with regards to real estate appraisal*. Real Estate Management and Valuation 30 (2022) 84-95. <https://doi.org/10.2478/remav-2022-0016>.
- [5] Chen JH., Su MC, Lin SK, Lin WJ, Gheisari M., *Smart bridge maintenance using cluster merging algorithm based on self-organizing map optimization*, Automation in Construction (2023) 104913, <https://doi.org/10.1016/j.autcon.2023.104913>.
- [6] Zhou Y., Sun L., *Effects of high winds on a long-span sea-crossing bridge based on structural health monitoring*, Journal of Wind Engineering & Industrial Aerodynamics 174 (2018) 260–268, <https://doi.org/10.1016/j.jweia.2018.01.001>.
- [7] Wang Q., Zheng Z., Qiao H., De Domenico D., *Seismic protection of reinforced concrete continuous girder bridges with inerter-based vibration absorbers*, Soil Dynamics and Earthquake Engineering 164 (2023) 107526, <https://doi.org/10.1016/j.soildyn.2022.107526>.
- [8] Czaplewski B., Bocian M., Macdonald J. H.G., *Calibration of inverted pendulum pedestrian model for laterally oscillating bridges based on stepping behaviour*, Journal of Sound and Vibration 572 (2024), 118141, <https://doi.org/10.1016/j.jsv.2023.118141>.
- [9] Samani F.S., Pellicano F., Masoumi A., *Performances of dynamic vibration absorbers for beams subjected to moving loads*. Nonlinear Dynamics 72 (2013), 1-2. DOI 10.1007/s11071-013-0853-4.
- [10] Luu M, Zabel V, Könke C., *An optimization method of multi-resonant response of high-speed train bridges using TMDs*. Finite Elements in Analysis and Design 53 (2012) 13–23, doi:10.1016/j.finel.2011.12.003
- [11] Herbut A., Rybak J., Brząkała W., *On a Sensor Placement Methodology for Monitoring the Vibrations of Horizontally Excited Ground*, Sensors 20 (2020), 1938; <https://doi.org/10.3390/s20071938>.
- [12] Ma R., Bi K., Hao H., *Inerter-based structural vibration control: A state-of-the-art review*, Engineering Structures 243 (2021) 112655, <https://doi.org/10.1016/j.engstruct.2021.112655>.
- [13] Konar, T., Ghosh, A.D., *Flow Damping Devices in Tuned Liquid Damper for Structural Vibration Control: A Review*. Archives of Computational Methods in Engineering 28 (2021) 2195–2207. <https://doi.org/10.1007/s11831-020-09450-0>.
- [14] Yang D-H., Shin J-H, Lee H.W., Kim S-K., Kwak M-K., *Active vibration control of structure by Active Mass Damper and Multi-Modal Negative Acceleration Feedback control algorithm*, Journal of Sound and Vibration, 392 (2017) 18-30. <https://doi.org/10.1016/j.jsv.2016.12.036>.
- [15] Shih M.H., Sung W.P., *Parametric Study of Impulse Semi-active Mass Damper with Developing Directional Active Joint*, Arabian Journal for Science and Engineering 46, (2021) 10711–10729. <https://doi.org/10.1007/s13369-021-05331-1>.
- [16] Billon, K., Zhao, G., Collette, C., Chesné, S. *Hybrid Mass Damper, Theoretical and Experimental Power Flow Analysis*, Journal of Vibration and Acoustics; 144 (4), (2022) 041003. <https://doi.org/10.1115/1.4053480>.
- [17] Antoniadis I.A., Kanarachos S.A., Gryllias K., Sapountzakis I.AE., *KDamping: A stiffness based vibration absorption concept*, Journal of Vibration and Control, Vol. 24 (2018) 588–606. <https://doi.org/10.1177/1077546316646514>.
- [18] Alexander N.A., Schilder F., *Exploring the performance of a nonlinear tuned mass damper*, Journal of Sound and Vibration, Volume 319 (2009) 445-462. <https://doi.org/10.1016/j.jsv.2008.05.018>.
- [19] Araz O; *Optimization of three-element tuned mass damper based on minimization of the acceleration transfer function for seismically excited structures*, Journal of the Brazilian Society of Mechanical Sciences and Engineering (2022) 44: 459, doi. [org/10.1007/s40430-022-03743-0](https://doi.org/10.1007/s40430-022-03743-0).
- [20] Prakash S., Jangid R. S., *Optimum parameters of tuned mass damper - inerter for damped structure under seismic excitation*, International Journal of Dynamics and Control (2022) 10:1322–1336 <https://doi.org/10.1007/s40435-022-00911-x>.
- [21] Shen Y., Peng H., Li X., Yang S., *Analytically optimal parameters of dynamic vibration absorber with negative stiffness*, Mechanical Systems and Signal Processing 85 (2017) 193–203, <https://doi.org/10.1016/j.ymsp.2016.08.018>.
- [22] Issa J.S., *Vibration absorbers for simply supported beams subjected to constant moving loads*. Proceedings of the Institution of Mechanical Engineers Part K Journal of Multi-body Dynamics 226(4) (2013) 398-404, <https://doi.org/10.1177/1464419312450652>.

- [23] Soong T.T., Grigoriu M., *Random vibration of mechanical and structural systems*, PTR Prentice-Hall, Inc, 1993.
- [24] Lin Y.K., Cai G.Q., *Probabilistic structural dynamics: Advanced theory and applications*, McGraw-Hill, 1995.
- [25] Samani F.S., Pellicano F., *Vibration reduction on beams subjected to moving loads using linear and nonlinear dynamic absorbers*. *Journal of Sound and Vibration* 325. (2009) 742-754. doi: 10.1016/j.jsv.2009.04.011.
- [26] Wang J.F., Lin C.C., Chen B.L., *Vibration suppression for high speed railway bridges using tuned mass dampers*, *International Journal of Solids and Structures* (2003) 40:465–491, [https://doi.org/10.1016/S0020-7683\(02\)00589-9](https://doi.org/10.1016/S0020-7683(02)00589-9).
- [27] Samani FS, Pellicano F, Masoumi A. *Performances of dynamic vibration absorbers for beams subjected to moving loads*, *Nonlinear Dynamics* 73(1-2) (2013),1065-79, DOI 10.1007/s11071-013-0853-4.
- [28] Adam C, Di Lorenzo S, Failla G, Pirrotta A. *On the moving load problem in beam structures equipped with tuned mass dampers*. *Meccanica* 52(13), (2017), 3101-15, DOI 10.1007/s11012-016-0599-4.
- [29] Pisal A. Y., Jangid R. S., *Vibration control of bridge subjected to multi-axle vehicle using multiple tuned mass friction dampers*, *International Journal of Advanced Structural Engineering* (2016) 8:213–227 DOI 10.1007/s40091-016-0124-y.
- [30] Podwórna M., Grosel J., *Optimisation of the parameters of a vibration damper installed on a historic bridge*. *Architecture Civil Engineering Environment*, 16, 4, pp. 93-101 (2023). <https://doi.org/10.2478/acee-2023-0053>.
- [31] Kahya V, Araz O., *Series multiple tuned mass dampers for vibration control of high-speed railway bridges*. In: Zingoni A (ed). *Insights and Innovations in Structural Engineering, Mechanics and Computation*. 1st ed. London: CRC Press, (2016) 143-148, DOI: 10.1201/9781315641645.
- [32] Wolfram Mathematica 13. Wolfram Research ©Copyright 1988-2023.
- [33] Araz O, Kahya V, *Optimization of multiple tuned mass dampers for a two-span continuous railway bridge via differential evolution algorithm*, *Structures* 39 (2022) 29–38, doi. org/10.1016/j.istruc.2022.03.021.
- [34] Storn R, Price K., *Differential evolution - a simple and efficient heuristic for global optimization over continuous spaces*, *Journal of Global Optimization* 11(4), (1997), 341–59, DOI10.1023/A:1008202821328.
- [35] Michalewicz Z., *Genetic Algorithm + Data Structures = Evolution Programs*, Springer-Verlag Berlin, 1992.
- [36] Goldberg, D. E., *Genetic algorithms in search, optimization, and machine learning*. Reading, MA: Addison-Wesley, 1989.
- [37] Grosel J., Podwórna M., *Optimisation of absorber parameters in the case of stochastic vibrations in a bridge with a deck platform for servicing pipelines*. *Studia Geotechnica et Mechanica* 43 (2021) 1–9. doi:10.2478/sgem-2021-0030.
- [38] Podwórna M., Grosel J., *Vibration absorber as a kind of reinforcement of a structure subjected to dynamic excitation*. *Materiały Budowlane (in polish)* (2022) DOI: 10.15199/33.2022.11.31.
- [39] Moghaddas M, Esmailzadeh E, Sedaghati R, Khosravi P., *Vibration control of Timoshenko beam traversed by moving vehicle using optimized tuned mass damper*, *Journal of Vibration and Control* 18(6), (2011), 757-73. DOI: 10.1177/1077546311404267.
- [40] Weber B., Feltrin G., *Assessment of long-term behaviour of tuned mass dampers by system identification*, *Engineering Structures* 32 (2010) 3670–3682. doi:10.1016/j.engstruct.2010.08.011.